A Single Point Mutation in the V3 Region Affects Protein Kinase Cα Targeting and Accumulation at Cell-Cell Contacts

ALICE VALLENTIN, THI-CHANG LO, AND DOMINIQUE JOUBERT*

INSERM U469, 34094 Montpellier Cedex 5, France

Given the importance of intercellular adhesion for many regulatory processes, we have investigated the control of protein kinase Cα (PKCα) targeting to the cell-cell contacts. We have previously shown that, upon treatment of the pituitary cell line GH3B6 with thyrotropin-releasing hormone (TRH) or phorbol 12-myristate 13-acetate (PMA), human PKCα (hPKCα) is selectively targeted to the cell-cell contacts (42). Here we show that the D294G mutation of hPKCα, previously identified in a subpopulation of human tumors, induces the loss of this selective targeting. The D294G mutant is instead targeted to the entire plasma membrane, including the cell-cell contacts, and the duration of the first rapid and transient translocation induced by TRH (42) is longer than that of the wild-type enzyme (93.3 versus 22.5 s), coinciding with the duration of the $[Ca^{2+}]_i$ increase. We found that in the presence or absence of PMA, RACK1 is never localized at the cell-cell contacts nor was it coimmunoprecipitated with hPKCα wild type or the D294G mutant. In contrast, PMA treatment or long-term TRH stimulation resulted in the presence of F-actin and β-catenin at the cell-cell contacts and their exclusion from the rest of the plasma membrane. Upon disruption of the F-actin network with phalloidin or cytochalasin D, wild-type hPKCα translocates but did not accumulate at the plasma membrane and β-catenin did not accumulate at the cell-cell contacts. In contrast, the disruption of the F-actin network affected neither translocation nor accumulation of the D294G mutant. These results show that the presence of PKCα at the cell-cell contacts is a regulated process which depends upon the integrity of both PKCα and the actin microfilament network.

Several years ago, we have shown that in a cell subpopulation of human pituitary and thyroid tumors, protein kinase Cα (PKCα) bore a point mutation at position 294, resulting in the substitution of an aspartic acid by a glycin (2, 31). The analysis of the biochemical properties of the D294G mutant and of the phenotype of embryonic fibroblasts stably transfected with it revealed a selective loss of recognition of substrates having characteristics of anchoring proteins (32) and a dramatic decrease in the dependence on serum growth factors for proliferation (3). In Rat6 fibroblasts stably transfected with human PKCα (hPKCα) or its mutant and treated with phorbol 12-myristate 13-acetate (PMA) for 1 h, the D294G mutant localized in the lysosome compartment (unpublished data), whereas wild-type hPKCα (hPKCα-wt) localized at the plasma membrane but not selectively at cell-cell contacts (3). Fibroblasts and epithelial cells are very different in many features. We therefore changed our model to the GH3B6 epithelial pituitary cell line. In this cell line, we found that PKCα is selectively targeted to the cell-cell contacts upon thyrotropin-releasing hormone (TRH) or PMA stimulation (42). To our knowledge, there is only one other study reporting on the presence of PKCα at the cell-cell contacts during spontaneous or PMA-induced compaction of the embryo (28). Inhibition of PKC activity blocks compaction, meaning that preventing PKCα localization at the cell-cell contacts resulted in an inappropriate cellular response (28). In view of the fact that an alteration in the cell-cell contacts is a hallmark of cell trans-formation and since PKCα might be involved in oncogenic transformation, localization of hPKCα at the cell-cell contact in GH3B6 cells, with no translocation in single cells (42), stimulated our interest. The goal of the present study was therefore to understand the mechanisms underlying the targeting of wild-type hPKCα to the cell-cell contact and to analyze the incidence of the D294G point mutation on hPKCα localization.

Epithelial cell-cell contacts involve extremely well-organized macromolecular structures. The transmembrane core of the adherence junction (localized at cell-cell contacts) is constituted by E-cadherin, which binds β-catenin, itself bound to α-catenin (4, 40). The actin cytoskeleton is linked to the adherence junction through its binding to α-catenin. Recently, Vasioukhin et al. have reported on the essential role of actin polymerization in the formation of adherence junction by demonstrating its role as a driving force for epithelial cell-cell adhesion (44). PKC is not an unknown actor in this dynamic process. It has indeed been shown to upregulate intercellular adhesion of α-catenin-negative human colon cancer cell variants via the induction of desmosomes (43). Several of its substrates, such as vinculin, are localized at cell-cell contacts (5, 13–15, 29, 38, 45). Glycogen synthetase kinase-3β, which phosphorylates β-catenin (16), is itself a PKC substrate (11). Concerning PKCα, besides being localized at cell-cell contacts during compaction (28), PKC is also known to interact directly or indirectly with the F-actin network. Two PKC isoforms, β and ε; possess actin-binding sites, and F-actin is able to directly stimulate PKC catalytic activity (7, 30, 39).

Localization of inactive PKC is essentially cytoplasmic. When stimulated, it interacts with membranes, including the plasma membrane, through at least two different mechanisms:

* Corresponding author. Mailing address: INSERM U469, 141 rue de la Cardonille, 34094 Montpellier Cedex 5, France. Phone: (33) 467-142-918. Fax: (33) 467-542-432. E-mail: joubert@u469.montp.inserm.fr.

a direct interaction with phospholipids (in particular phosphatidylserin) or an indirect interaction via anchoring proteins such as RACK1 (receptor for activated kinase C 1). It has been suggested that a progressive decrease in the level of RACK1 is responsible for the decrease in PKC accumulation at the plasma membrane observed in the process of aging (6). RACK1 has also been suggested to be an intracellular PKC shuttling protein for PKCβII (34). Although it is generally accepted that an increase in intracellular calcium concentration ($[Ca^{2+}]_i$) is sufficient to induce PKCα translocation, we have shown that this is not the case in the GH3B6 cells since translocation occurs only in contacting cells despite the similar increase in $[Ca^{2+}]_i$ registered in all stimulated cells, whether single or apposed (42). We thus hypothesized the existence of additional levels of control that drive PKCα to its targeting site and further allow its accumulation. Several candidates could be involved, including RACK1 and F-actin.

We show here that cell-cell contact targeting is highly regulated since, in the presence of the D294G point mutation, hPKCα accumulates at the entire plasma membrane, including the cell-cell contacts. On the basis of the lack of colocalization or coimmunoprecipitation of RACK1 with hPKCα, we think RACK1 is not involved in the cell-cell contact targeting. In contrast, we present evidence for an involvement of F-actin in wild-type hPKCα accumulation. Furthermore, we show that polymerization of acting at the cell-cell contacts correlates with the accumulation of β-catenin at this location upon PMA treatment or long-term TRH stimulation, both partners being thus colocalized with PKCα.

MATERIALS AND METHODS

Materials. PMA, histone IIIS, phalloidin, cytochalasin D, goat anti-mouse immunoglobulin M (IgM; μ-chain specific)-agarose beads, goat anti-rabbit IgG-tetramethyl rhodamine isocyanate (TRITC), and phosphatidylserine were purchased from Sigma (Saint Quentin Fallavier, France). Restriction enzymes were from Promega (Charbonnières, France). *Taq* DNA polymerase, Ham F-10 and horse serum were from Eurobio (Les Ulis, France). ExGen 500 (linear polyethyleneimine) and monoclonal anti-PKCα antibody were from Euromedex (Souffelweyersheim, France). Fetal bovine serum was from BioWhittaker (Walkersville, Md.). Monoclonal antibody against green fluorescent protein (GFP), 1-*O*-*n*-octyl-β-D-glucopyranoside, anti-mouse IgG-peroxidase, Fab fragments, and chemiluminescence detection kit were from Roche Molecular Biochemicals (Indianapolis, Ind.). pEGFP-N1 plasmid was from Clontech (Palo Alto, Calif.). The cDNA clones coding for wild type (hPKCα-wt) or mutant D294G (hPKCα-D294G) of PKCα were provided by V. Alvaro and B. I. Weinstein from Columbia Cancer Center, New York, N.Y. Protein G-agarose and anti-β-catenin antibody were from Santa Cruz Biotechnology, Inc. (Santa Cruz, Calif.). [γ-^{32}P] ATP, sheep anti-mouse immunoglobulin horseradish peroxidase-linked antibody, and membrane Hybond C-Extra were from Amersham Pharmacia Biotech (Les Ulis, France). Monoclonal anti-RACK1 antibody was purchased from Transduction Laboratories (Lexington, Ky.). Phalloidin-TRITC was from Molecular Probes (Eugene, Oreg.). Goat anti-rabbit IgG (H+L), horseradish peroxidase conjugated, was from Pierce (Rockford, Ill.). TRH was from Calbiochem (Meudon, France). Anti-mouse IgM-TRITC was from Nordic Immunological Laboratories. Goat anti-mouse IgG-TRITC was from Jackson ImmunoResearch (Marseille, France).

Construction of plasmids encoding fusion proteins. The GFP fusion proteins used in transient-transfection experiments are schematically represented in Fig. 1A. The hPKCα-wt or hPKCα-D294G cDNA with an *Eco*RI site at their 5′ terminus and a *Kpn*I site at their 3′ terminus were produced by PCR using wild-type or mutant D294G hPKCαcDNA subcloned into pBabe vectors as templates.

The sense and antisense primers used to generate these constructs were GGAATTCCGGAGCAAGAGGTGGTT and GGGGTACCCCTACTGCACT CTGTAAGAT, respectively. The cycle parameters were 94°C for 1 min, 54°C for 2 min, and 72°C for 3 min.

The PCR fragments encoding hPKCα-wt or hPKCα-D294G were gel purified, digested with *Eco*RI and *Kpn*I, and then fused in frame to GFP by ligation into *Eco*RI- and *Kpn*I-digested pEGFP-N1 vector. The sequences of ligated PCR fragments were checked by DNA sequencing, and no mutations were detected.

Cell culture, transfection, and observation of fusion protein localization in living cells. GH3B6 cells were cultured in Ham F10 medium supplemented with 2.5% (vol/vol) fetal bovine serum and 15% (vol/vol) horse serum, both of which were heat inactivated at 56°C for 1 h. Transient transfection of GH3B6 cells was performed with ExGen as described previously (42). The localization of fusion proteins in living cells was examined by conventional (PMA treatment) or confocal (TRH treatment) fluorescence microscopy. The confocal laser scanning microscope was equipped with an Ar/Kr laser (Odyssey XL with InterVision 1.4.1 software; Noran Instruments, Inc., Middleton, Wis.) as described by Guérineau et al. (12). At the time of observation, the culture medium was replaced by a buffer containing 140 mM NaCl, 5 mM KCl, 2 mM CaCl₂, 2 mM MgCl₂, 10 mM HEPES, and 6 mM glucose (pH 7.4).

PKCα, RACK1, F-actin, and β-catenin detection by immunocytochemistry. GH3B6 cells were seeded on 20-by-20-mm² coverslips in 2.5 ml of Ham F10 medium and grown for 24 h before transfection or immunocytochemistry. Cells were washed quickly three times with phosphate-buffered saline (PBS; 140 mM NaCl, 27 mM KCl, 8 mM Na₂HPO₄, 1.5 mM KH₂PO₄), fixed for 1 min with 3% formaldehyde (vol/vol) in PEM buffer (80 mM PIPES, 5 mM EDTA, 2 mM MgCl₂; pH 6.5), and treated for 8 additional min with 3% formaldehyde (vol/vol) in 100 mM sodium borate at pH 11. Cells were incubated for 15 min in PBS containing 0.1% (wt/vol) sodium borohydride, washed, permeabilized by incubation in PBS supplemented with 0.2% Triton X-100, washed, incubated for 30 min with TBS (10 mM Tris, 150 mM NaCl; pH 7.6) containing 1% bovine serum albumin, and washed again. Cells were then incubated overnight at 4°C with antibodies against PKCα, RACK1, or β-catenin (dilution, 1:100) and washed. Cells were further incubated for 60 min with phalloidin-TRITC for F-actin labeling or with the second antibody, i.e., goat anti-mouse IgG-TRITC (diluted 1:40), goat anti-mouse IgM TRITC (diluted 1:40), or goat anti-rabbit IgG TRITC (diluted 1:125) for PKCα, RACK1, or β-catenin immunostaining, respectively. After being washed, cells were postfixed for 15 min with 3% formaldehyde in PBS and incubated in the presence of 50 mM NH₄Cl for 10 min. Coverslips were mounted in 1,4-diazabicyclo-[2.2.2]octane at 100 mg/ml in PBS containing 50% glycerol. Subcellular localization of fluorescence was examined by conventional fluorescence microscopy.

Immunoprecipitation of hPKCα-wt–GFP and hPKCα-D294G–GFP. hPKCα-wt–GFP or hPKCα-D294G–GFP constructs were transiently transfected into GH3B6 cells. At 48 h after transfection, cells were washed in cold PBS and incubated in radioimmunoprecipitation assay buffer (50 mM Tris, pH 7.4; 150 mM NaCl; 1% Nonidet P-40; 0.25% sodium deoxycholate; 1 mM EGTA; 1 mM phenylmethylsulfonyl fluoride [PMSF]; 1 μg of aprotinin, 10 μg of leupeptin, and 1 μg of pepstatin per ml; 1 mM sodium orthovanadate) at 4°C by gentle rocking. Cells were then scraped and collected into microcentrifuge tubes. Lysates were precleared with 20 μl of protein G beads, incubated for 10 min at 4°C by gentle rocking, and centrifuged at 14,000 × *g* for 10 min at 4°C. Supernatants were collected. Then, 2 mg of the cell proteins was mixed with 2 μg of GFP antibody, and the reaction mixture was incubated at 4°C overnight. Immunocomplexes were captured by adding 20 μl of protein G beads. This mixture was gently rocked at 4°C overnight. After centrifugation and washing of the beads with 800 μl of 50 mM Tris (pH 7.4) supplemented with 1 μg of aprotinin, 1 μg of leupeptin, and 1 μg of pepstatin per ml, immunocomplexes were either resuspended in 50 μl of 50 mM Tris (pH 7.4) for further kinase activity assay or in 50 μl of Laemmli buffer (19) for Western blot analysis.

PKCα catalytic activity measurement. Catalytic activity of immunoprecipitated hPKCα-wt–GFP or hPKCα-D294G–GFP were measured with histone IIIS as a substrate. The amount of each protein used for catalytic activity assay was estimated before the assay by Western blot analysis with a GFP antibody.

Activity was measured in the presence of 20 μM histone IIIS, 1 μM EGTA, 10 μM PMA, 5 mM magnesium acetate, 25 μM ATP, 1 mM dithiothreitol, 1 nM [γ-^{32}P]ATP (specific activity, 30 Ci/mmol) (Amersham), an 10 μg of phosphatidylserine per ml (3). The reaction was prepared in the absence or presence of 1.2 mM calcium. Reaction was started by incubation at 30°C for 5 min and stopped at 0°C for 5 min. A half-volume of each reaction mixture was dropped down on phosphocellulose paper P81 (Whatman) squares which were subsequently washed twice for 10 min in 0.01 M phosphoric acid, once in acetone for 30 s, once in petroleum ether for 10 s and then air dried. The paper squares were transferred to scintillation vials and counted.

Coimmunoprecipitation. At 48 h after transfection, cells transfected with hPKCα-wt–GFP or hPKCα-D294G–GFP were incubated for 60 min with either fresh media or 100 nM PMA. Cells were washed in cold PBS and lysed at 4°C in 50 mM Tris-HCl (pH 7.5) containing 150 mM NaCl; 1% 1-*O*-*n*-octyl-β-D-gluco-

pyranoside; 1 mM EGTA; 1 mM PMSF; 1 μg of aprotinin, 10 μg of leupeptin, and 1 μg of pepstatin per ml; and 1 mM sodium orthovanadate. Lysed cells were centrifuged at $14,000 \times g$ for 10 min at 4°C. Supernatants were collected, and immunoprecipitation with anti-GFP or anti-RACK1 antibodies was performed. Briefly, the antibodies used were cross-linked to either protein G-agarose for GFP antibody or anti-mouse IgM-agarose beads for RACK1 antibody. The cross-linked antibodies (2 μg of anti-GFP or 2.5 μg of anti-RACK1) were incubated with 2 mg of cell lysates for 90 min on ice. The beads were washed thoroughly. Proteins were removed from beads by incubation for 5 min at 95°C in 20 μl of Laemmli buffer for Western blot analysis. These samples were subjected to sodium dodecyl sulfate-polyacrylamide gel electrophoresis (SDS-PAGE) on a 10% polyacrylamide gel, and transferred onto nitrocellulose membranes. Membranes were cut at approximately the migration front of the 50-kDa proteins and probed either with anti-GFP antibody (1:500) in order to detect hPKCα-GFP at 103 kDa or with anti-RACK1 antibody (1:1,000) in order to detect RACK1 at 36 kDa. After being washed, the membranes were incubated for 1 h at room temperature with anti-mouse IgG-peroxidase antibody (1:4,000) for GFP staining or with anti-mouse immunoglobulin-peroxidase (1:2,000) for the detection of RACK1. Immunoreactive bands were visualized with the chemiluminescence detection kit.

Cell fractionation and Western blot analysis. Untransfected or transiently transfected GH3B6 cells were separated into soluble and membrane fractions. Cells were washed with cold PBS followed by scraping into homogenization buffer (10 mM Tris; 2 mM EDTA; 1 mM PMSF; 1 μg of aprotinin, 10 μg of leupeptin, and 1 μg of pepstatin per ml; 1 mM sodium orthovanadate). Cells were then homogenized in a glass Dounce homogenizer and centrifuged for 30 min at 14,000 rpm. Supernatants were collected; they corresponded to the soluble fractions. Pellets were resuspended in homogenization buffer supplemented with 1% (vol/vol) Nonidet P-40 and incubated for 45 min on ice. This corresponds to the membrane fractions.

For immunoblotting, soluble and membrane fractions were subjected to SDS-PAGE and electrophoretically transferred onto nitrocellulose membranes. Nonspecific binding sites were blocked by incubation with TBS (50 mM Tris, 150 mM NaCl; pH 7.4) containing 10% powdered milk for 1 h at room temperature. Membranes were then incubated with anti-PKCα (1:2,000), anti-GFP (1:1,000), anti-RACK1 (1:2,500), or anti-β-catenin (1:400) antibody overnight at 4°C. After being washed with TBS containing 0.1% Tween, the membranes were incubated for 1 h at room temperature with anti-mouse IgG-peroxidase antibody (1:4,000) for PKCα and GFP staining and with anti-mouse immunoglobulin-peroxidase (1:2,000) or anti-rabbit IgG-peroxidase (1:4,000) for the detection of RACK1 and β-catenin, respectively. Immunoreactive bands were visualized with the chemiluminescence detection kit.

Intracellular calcium concentration changes. The cytoplasmic free calcium concentration ($[Ca^{2+}]_i$) were measured with a real-time confocal laser scanning microscope (12). Cells were visualized with a 63-by-0.9 numerical aperture achroplan water immersion objective lens (Zeiss). The larger slit (100 μm) was used, giving bright images with a 3.1-μm axial resolution. Cells were loaded with the Ca^{2+}-sensitive fluorescent probe Fluo-3 by exposure to 50 μM Fluo-3 acetoxymethyl ester (Fluo-3/AM; Molecular Probes) by incubation for 30 min at 37°C in a humidified incubator. Fluo-3 was excited through a 488-nm band-pass filter, and the emitted fluorescence was collected through a 515-nm barrier filter. $[Ca^{2+}]_i$ changes were expressed as the F/F_{min} ratio where F_{min} was the minimum fluorescent intensity measured during the recording (30 images/s). Acquired data were then processed for analysis using Igor 3.14 (Wavemetrics, Inc., Lake Oswego, Oreg.) softwares. Three separate experiments were performed, and a minimum of 10 fields per experiment with both single and contacting cells were analyzed for $[Ca^{2+}]_i$ changes.

RESULTS

The natural D294G mutation abolishes the specific targeting of hPKCα to cell-cell contacts upon PMA stimulation. In order to determine whether PKCα localization is affected by the D294G mutation, we transiently transfected GH3B6 cells with expression plasmids for the two hPKCα-wt–GFP and hPKCα-D294G–GFP fusion proteins (Fig. 1A). We then visualized the subcellular distribution of each fusion protein in live GH3B6 cells under basal conditions or after PMA stimulation. The pattern of GFP immunofluorescence recorded in living GH3B6 cells observed under a confocal microscope reflects

the spatiotemporal dynamics of translocation of hPKCα-wt–GFP and hPKCα-D294G–GFP. As shown in Fig. 1B, the location of both hPKCα-wt–GFP and hPKCα-D294G–GFP was cytoplasmic in unstimulated cells, whether isolated or apposed. Upon stimulation with 100 nM PMA for 60 min, hPKCα-wt–GFP (and endogenous PKCα, results already published [42]) was selectively targeted to cell-cell contacts in apposed cells and was not translocated in isolated cells, as previously shown (42). In contrast, under the same conditions, the hPKCα-D294G mutant translocated uniformly, cell-cell contacts included, to the plasma membrane of stimulated cells, whether single or apposed. Therefore, whereas the D294G mutation does not affect cytoplasmic localization under basal conditions, the specific localization at the interface of apposed cells is lost after PMA activation.

Although we had previously demonstrated that the GFP tag does not alter the catalytic activity of wild-type hPKCα (42), we wanted to ensure that this was also the case for hPKCα-D294G. We thus compared the kinase activities of hPKCα-D294G–GFP and hPKCα-wt–GFP. Both fusion proteins were immunoprecipitated from transiently transfected GH3B6 cells. Their catalytic activities were measured in the presence of PMA and phosphatidylserine, with or without Ca^{2+} using histone IIIS as substrate. As shown in Fig. 1C, the catalytic activities of both proteins were similar and were increased upon Ca^{2+} addition. Figure 1C also shows that similar amounts of both proteins were immunoprecipitated and used for catalytic activity measurements.

Different mechanisms underly translocation of the wild-type and the D294G mutant forms of hPKCα. In our previous work, we observed that stimulation of GH3B6 cells by TRH induces a biphasic accumulation of hPKCα at the plasma membrane (42). We also provided evidence that the mechanisms which underlie the early and transient phases of translocation induced by TRH are different from those involved in the longer, second phase that follows long-term treatment with TRH or PMA. Here, we investigated whether the presence of the D294G mutation affects hPKCα translocation after short-term treatment with TRH as is the case after PMA stimulation. As shown in Fig. 2A, TRH application induced the rapid and transient translocation of the wild-type protein exclusively at the interface between cells. Under the same conditions, the D294G mutant also translocated (Fig. 2B), but its translocation was also observed in single cells (Fig. 2B), the selective translocation to cell-cell contacts being lost (data not shown), as is the case with PMA treatment, and the time the D294G mutant remained at the plasma membrane was longer (93.3 versus 22.5 s) (Fig. 2C). These results suggest that the mechanisms involved in the accumulation of the D294G mutant and the wild-type form of the enzyme at the plasma membrane are different.

A rise in the intracellular calcium concentration ($[Ca^{2+}]_i$) is known to be necessary for conventional PKC translocation. We have previously shown that (i) hPKCα does not translocate in isolated GH3B6 cells treated with TRH in spite of the observed concomitant rise in $[Ca^{2+}]_i$ (42) and (ii) in apposed cells, hPKCα returns to the cytoplasm very rapidly despite the still elevated $[Ca^{2+}]_i$ (Fig. 2C). The duration of the first translocation phase is significantly longer in cells expressing the mutant compared to cells expressing the wild-type enzyme. We
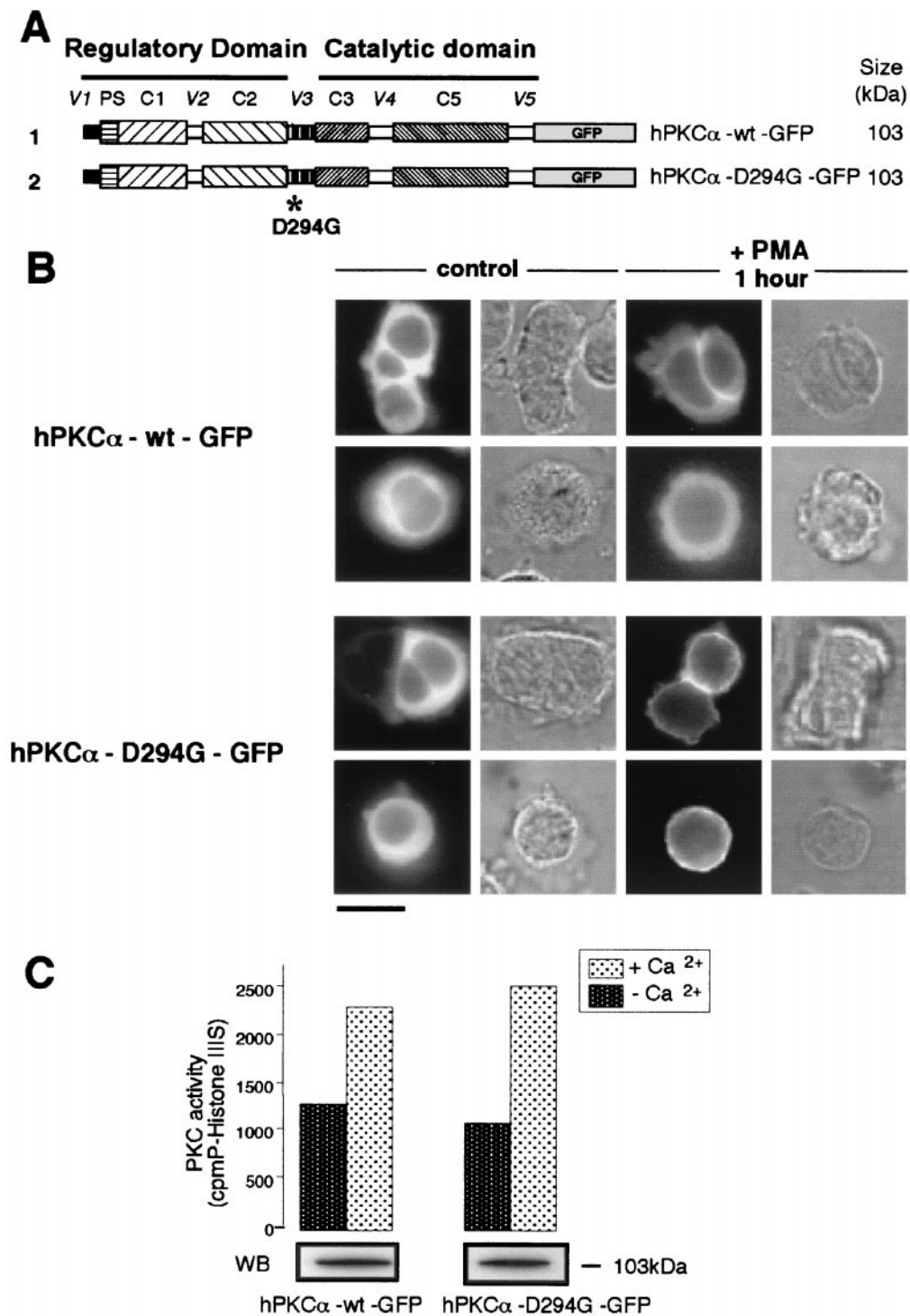
FIG. 1. The presence of the natural D294G mutation abolishes the specific targeting of hPKCα at the interface between apposed cells upon PMA stimulation. (A) Schematic representation of hPKCα-wt–GFP and hPKCα-D294G–GFP fusion proteins with their expected molecular weights. As described in Materials and Methods, hPKCα-wt and hPKCα-D294G cDNA were subcloned in frame at the 5′ end of the sequence encoding GFP with EcoRI and KpnI sites. The D294G point mutation is localized in the V3 hinge region of hPKCα. (B) Localization of hPKCα-wt–GFP (top) and hPKCα-D294G–GFP (bottom) observed in transiently transfected living GH3B6 cells. In basal conditions, hPKCα-wt–GFP and hPKCα-D294G–GFP are both cytoplasmic. When cells are treated with 100 nM PMA for 1 h, hPKCα-wt–GFP is exclusively targeted at the interface between apposed cells. In contrast, in the same conditions, hPKCα-D294G–GFP is uniformly targeted at the plasma membrane of apposed cells and of isolated cells. Bar, 5 μm. (C) The GFP tag does not affect the activity of hPKCα-D294G. PKC catalytic activity was assessed by measuring the incorporation of ^{32}P from [γ-^{32}P]ATP into histone IIIS substrate in the presence of 10 μg of phosphatidylserine per ml and 10 μM PMA. The experiment was performed in the presence or in the absence of 1.2 mM calcium. Results show that histone IIIS is equally phosphorylated by hPKCα-wt–GFP and hPKCα-D294G–GFP. Western blot analysis of immunoprecipitated hPKCα-wt–GFP and hPKCα-D294G–GFP (revealed with the anti-GFP antibody) indicates the amount of each protein used for PKC activity assay. Three separate experiments gave identical results.
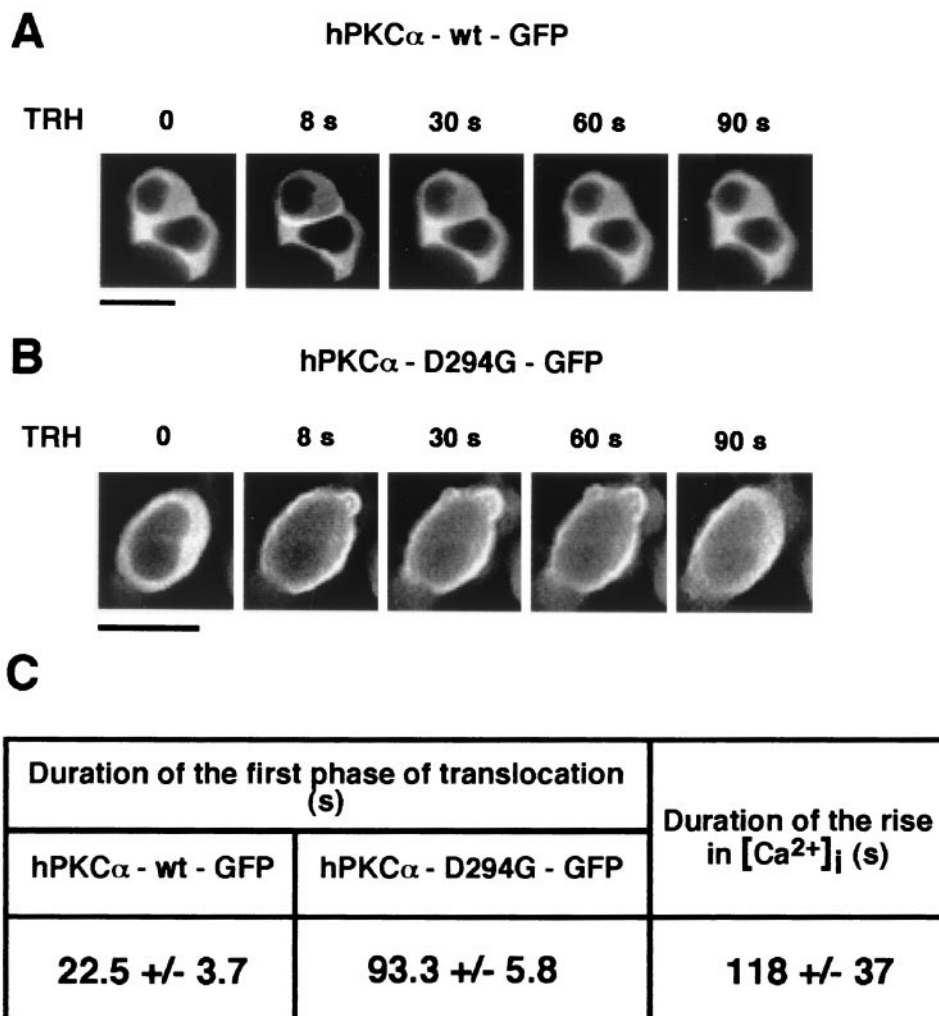
A   hPKCα - wt - GFP

B   hPKCα - D294G - GFP

C

Duration of the first phase of translocation (s)		Duration of the rise in $[Ca^{2+}]_i$ (s)
hPKCα - wt - GFP	hPKCα - D294G - GFP	
22.5 +/- 3.7	93.3 +/- 5.8	118 +/- 37

FIG. 2. Time course of plasma membrane translocation of hPKCα-wt–GFP and hPKCα-D294G–GFP upon TRH stimulation. (A and B) GH3B6 cells expressing hPKCα-wt–GFP (A) or hPKCα-D294G–GFP (B) were observed with a confocal microscope immediately before and during stimulation with 100 nM TRH. Images were recorded every 2 s for 3 min. Translocation was observed for the two proteins as soon as 8 s after the beginning of stimulation. As upon PMA stimulation, hPKCα-D294G–GFP lost the selective targeting to the cell-cell contacts. Indeed, as observed in this single cell (B), hPKCα-D294G–GFP translocated uniformly at the plasma membrane. Although TRH-induced translocation was reversible for both proteins, hPKCα-D294G–GFP remained at the plasma membrane for a longer time than the wild-type enzyme. Bar, 5 μm. (C) Duration of the translocation of hPKCα-wt–GFP and hPKCα-D294G–GFP and of the increase in $[Ca^{2+}]_i$ induced by TRH stimulation. The cytosolic variations in $[Ca^{2+}]_i$ were recorded using real-time scanning laser confocal imaging. Cells were loaded with 50 μM Fluo-3/AM for 30 min at 37°C, and the variation in F/F_{min} values was calculated from the recorded fluorescence of the cells. Values are given as the mean ± the standard deviation. Duration of wild-type enzyme translocation is statistically different from that of the mutant ($P < 0.005$) and different from duration of $[Ca^{2+}]_i$ increase ($P < 0.0002$). The duration of mutant translocation is not statistically different from duration of the $[Ca^{2+}]_i$ rise ($P > 0.8$).

thus compared the duration of translocation of the mutant and $[Ca^{2+}]_i$ rise upon TRH stimulation. As shown in Fig. 2C, the $[Ca^{2+}]_i$ was elevated for 118 ± 37 s, a duration that is not statistically different from the time hPKCα-D294G remained at the plasma membrane (93.3 ± 5.8 s). In contrast, this duration is statisically different from the time wild-type hPKCα remained at the cell-cell contacts (22.5 ± 3.7 s). These results suggest the existence of different mechanisms of interaction for the mutant and the wild-type enzyme with the plasma membrane and cell-cell contacts, respectively, one being probably dependent upon the $[Ca^{2+}]_i$ and the other not.

RACK1 is not involved in hPKCα-wt or hPKCα-D294G localization. It has been proposed that localization of PKC could be in part mediated by interactions with anchoring proteins, including RACK1. In order to determine whether RACK1 is the partner involved in the translocation and/or accumulation of activated PKCα, we analyzed by Western blot, immunocytochemistry, and coimmunoprecipitation whether or not RACK1 could colocalize and interact with hPKCα-wt and hPKCα-D294G.

The Western blot shown in Fig. 3A demonstrates that under basal conditions, RACK1 is found both in the soluble and and in the membrane fractions. In addition, whereas PMA treatment induced the expected translocation of hPKCα-wt as attested by the decreased signal in the soluble fraction and the concomitant increase in the membrane fraction, it had no significant effect on the distribution of RACK1 in both fractions. The prominent RACK1 immunoreactivity observed at
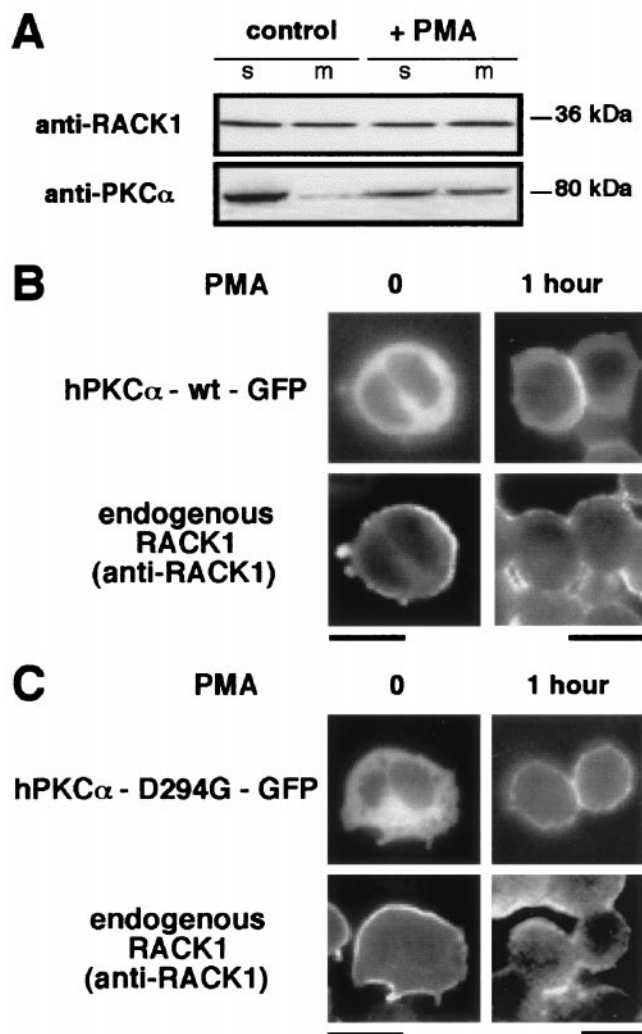
FIG. 3. RACK1 localization upon basal condition or PMA stimulation. (A) Western blot analysis of RACK1 and PKCα distribution. Soluble (s) and membrane (m) fractions of untreated or PMA-treated GH3B6 cells were subjected to SDS-PAGE and Western blot using anti-RACK1 or anti-PKCα antibodies. In basal conditions, RACK1 was found in soluble and membrane fractions. PMA treatment has no significant effect on RACK1 distribution, whereas it induced the expected translocation of PKCα, as evidenced by the increased PKCα immunoreactivity in the membrane fraction. (B and C) GH3B6 cells transfected with hPKCα-wt–GFP (B, top) or hPKCα-D294G–GFP (C, top) were analyzed for RACK1 localization by immunocytochemistry with an anti-RACK1 antibody (B and C, bottom) in basal conditions (left) and after 1 h of PMA treatment (right). Under basal conditions, RACK1 immunoreactivity was found mainly at the plasma membrane but not at the cell-cell contacts. PMA stimulation did not affect RACK1 localization. As already shown in Fig. 1, hPKCα-wt–GFP and hPKCα-D294G–GFP were cytoplasmic in basal conditions. Upon PMA stimulation, hPKCα-wt–GFP translocated at the interface of apposed cells, whereas hPKCα-D294G–GFP translocated uniformly at the plasma membrane. Bars, 5 μm

the plasma membrane of apposed cells at the exclusion of cell-cell contact (Fig. 3B) remained unchanged upon PMA stimulation, whereas in the same cells, hPKCα-wt–GFP specifically translocated to the interface of apposed cells. Upon long-term TRH stimulation, RACK1 did not relocalize (data not shown). This observation suggested that RACK1 may not be the an-

choring protein involved in hPKCα-wt translocation or accumulation at the interface of apposed cells. In apposed cells transiently tranfected with hPKCα-D294G–GFP treated or not with PMA (Fig. 3C), the RACK1 localization was similar to that of apposed cells transfected with the wild-type hPKCα, i.e., excluded from the cell-cell contact, thus resulting in the partial colocalization of the D294G mutant and RACK1 at the plasma membrane after PMA treatment. In isolated cells, RACK1 and hPKCα-D294G–GFP were totally colocalized (data not shown).

Coimmunoprecipitation experiments were then undertaken in order (i) to ensure that there was no interaction between RACK1 and the wild-type form of hPKCα and (ii) to investigate whether the colocalization of hPKCα-D294G–GFP with RACK1 involved or not an interaction between the two proteins. The results shown in Fig. 4 demonstrate that RACK1 was absent from hPKCα-wt–GFP immunoprecipitates (Fig. 4A) and that hPKCα-wt–GFP was absent from RACK1 immunoprecipitates (Fig. 4B), Whether GH3B6 cells were treated or not with PMA. The same was true for extracts of cells expressing the D294G mutant form of hPKCα (Fig. 4A and B). Thus, we conclude that in GH3B6 cells, neither hPKCα nor hPKCα-D294G interacts with RACK1 in vivo upon PMA stimulation. Similarly, we did not detect the endogenous PKCα in RACK1 immunoprecipitates (data not shown). The Western blot shown in Fig. 4C, performed with the cell extracts used for immunoprecipitation, demonstrates that the failure to detect RACK1 in GFP immunoprecipitates cannot be imputed to a flaw in our detection technique. Furthermore, we used several experimental procedures, including that of Tony Ng (Peter Parker's laboratory), who succeeded in coimmunoprecipitating RACK1 and PKCα in a different cell type, (unpublished result).

Wild-type hPKCα accumulation at cell-cell contacts depends on the reorganization of F-actin. Since there is evidence from the literature that F-actin may interact with some PKCs and modulate their catalytic activities (7, 30, 39) and since F-actin is intimately linked with the molecular complexes present at cell-cell contacts, we investigated whether endogenous F-actin participates in the localization of hPKCα. To this end, F-actin was labeled with phalloidin-TRITC in cells transfected with hPKCα-wt–GFP. In the absence of PMA, F-actin was found to be uniformly distributed at the plasma membrane, whereas hPKCα-wt–GFP was as expected found in the cytoplasm (Fig. 5A). After 1 h of PMA stimulation, F-actin and endogenous PKCα concomitantly accumulated at the plasma membrane of apposed cells. A kinetic analysis of the effect of PMA on F-actin reorganization showed that the effect started at 10 min and lasted for at least up to 1 h of treatment (data not shown).

Colocalization of F-actin and hPKCα upon PMA treatment indicated that F-actin may participate in hPKCα translocation and/or accumulation at cell-cell contacts. We thus treated transiently transfected cells with phalloidin that blocks actin polymerization or cytochalasin D, which induces the breakdown of actin filaments. The consequences of such treatments on hPKCα translocation or accumulation were analyzed by the technique of Western blot. In living GH3B6 cells incubated for 1 h with phalloidin-TRITC in the medium, the actin network was found to be disorganized (Fig. 5B). Phalloidin-TRITC staining was performed on fixed 0.5 μM cytochalasin D-treated
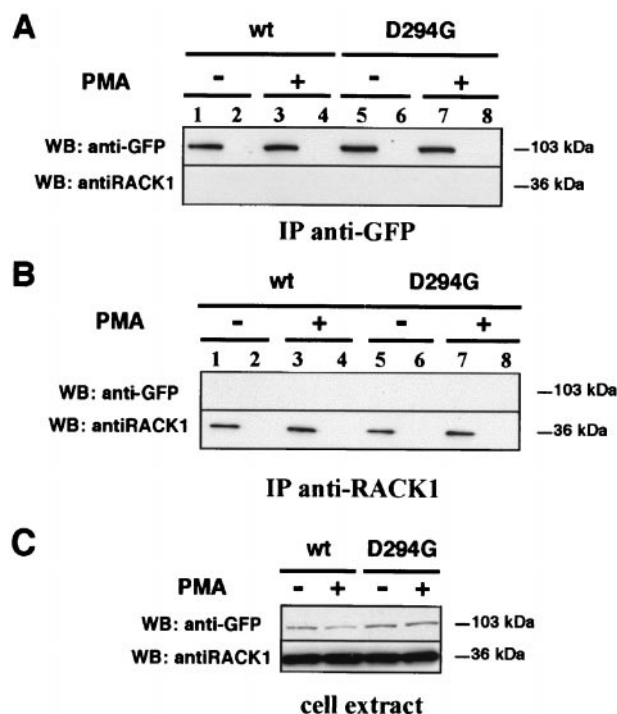
FIG. 4. RACK1 interacts neither with hPKCα-wt nor with hPKCα-D294G. GH3B6 cells transfected with hPKCα-wt–GFP or hPKCα-D294G–GFP were treated or not treated with 100 nM PMA and then lysed for a coimmunoprecipitation experiment by using anti-GFP or anti-RACK1 antibodies as described in Materials and Methods. For Western blot analysis, membranes were cut at approximately the migration front of the 50-kDa proteins and probed either with anti-GFP antibody in order to detect hPKCα-GFP at 103 kDa or with anti-RACK1 antibody in order to detect RACK1 at 36 kDa. (A and B) Immunoprecipitation experiment with anti-GFP antibody or with anti-RACK1 antibody. Anti-RACK1 antibody (B) or anti-GFP antibody (C) was incubated with untreated cells (lanes 1 and 5) or PMA-treated cells (lanes 3 and 7). Protein G alone was incubated with untreated cells (lanes 2 and 6) or PMA-treated cells (lanes 4 and 8). Samples were analyzed by Western blot using anti-GFP and anti-RACK1 antibodies. When RACK1 was immunoprecipitated from untreated (B, lanes 1 and 5) or PMA-treated (B, lanes 3 and 7) cells, neither hPKCα-wt–GFP nor hPKCα-D294G–GFP was coimmunoprecipitated. When hPKCα-wt–GFP or hPKCα-D294G–GFP were immunoprecipitated from untreated (C, lanes 1 and 5) or PMA-treated (C, lanes 3 and 7) cells, RACK1 was never coimmunoprecipitated. (C) Western blot analysis of RACK1 (bottom, lanes 1 to 4), hPKCα-wt–GFP (top, lanes 1 and 2), and hPKCα-D294G–GFP (top, lanes 3 and 4) expression in cell extracts of untreated (lanes 1 and 3) or PMA-treated (lanes 2 and 4) cells used for coimmunoprecipitation experiment.

cells (30 min) in order to verify that such a treatment on GH3B6 cells had the expected consequences on F-actin network. Figure 5B shows that this was indeed the case.

In the absence of PMA stimulation and with or without phalloidin pretreatment, PKCα is mainly found in the soluble fraction (Fig. 5C). In cells not preincubated with phalloidin, PMA stimulation (from 10 to 90 min) induced a decrease of the soluble fraction immunoreactivity that correlated with an increase in that of the membrane fraction (Fig. 5C, left). This increase persisted for up to 90 min of PMA stimulation. When cells were preincubated with phalloidin, the PKCα level also increased in the membrane fraction from 10 to 20 min of PMA stimulation, indicating that translocation had occurred. Sur-

prisingly, during the period from 40 to 90 min of PMA treatment, the PKCα level decreased in the membrane fraction, whereas it increased in the soluble fraction and finally returned to a basal level (Fig. 5B, right). The same results were obtained with cells preincubated with cytochalasin D before PMA stimulation (Fig. 5D). Thus, when the F-actin network is disrupted with either phalloidin or cytochalasin D, long-lasting accumulation of PKCα at the plasma membrane cannot occur, whereas translocation can. Therefore, F-actin accumulation at cell-cell contacts upon PMA stimulation seems to be necessary for the biological activity of hPKCα at cell-cell contacts.

The D294G point mutation abolishes the F-actin dependence of hPKCα accumulation. The D294G point mutation abolishes the selectivity of hPKCα targeting to cell-cell contacts. Considering the colocalization of F-actin with wild-type hPKCα upon PMA stimulation and the effect of the F-actin network reorganization on wild-type hPKCα accumulation, we analyzed the link between the F-actin network and translocation of accumulation of the hPKCα-D294G mutant.

Phalloidin-TRITC staining of cells transiently transfected with hPKCα-D294G–GFP indicated that the expression of the mutant did not affect reorganization of the F-actin network at the cell-cell contacts upon PMA treatment (Fig. 6A). Western blot analysis indicated that phalloidin (Fig. 6B) or cytochalasin D (data not shown) pretreatment did not affect translocation or accumulation of the hPKCα-D294G–GFP fusion protein. Indeed, in cells that were preincubated or not for 1 h with phalloidin and stimulated with PMA from 10 to 60 min, we observed the same decrease of the soluble fraction immunoreactivity that correlated to an increase in the membrane fraction immunoreactivity. In both experimental conditions, this increase persisted in the membrane fraction during the entire time of the PMA treatment. Thus, the different subcellular localizations of the wild-type hPKCα and mutant hPKCα-D294G at the plasma membrane may involve not only different targeting mechanisms but also different mechanisms of interaction with the membrane.

β-Catenin accumulates at cell-cell contacts upon PMA stimulation. Cadherins are proteins specialized in cell-cell adhesion and are associated with β-catenin that mediates a link between cadherins and the actin-cytoskeleton via α-catenin. During embryonic compaction, it has been demonstrated that β-catenin and PKCα are both colocalized at the cell-cell contacts of apposed cells (28). The same study provided evidence for a role of PKC in the phosphorylation of β-catenin. This led us to investigate whether β-catenin was colocalized with PKCα at the cell-cell contacts under PMA stimulation. The endogenous β-catenin and PKCα localization was determined by Western blot and immunocytochemistry in basal conditions and upon PMA treatment.

As determined by the technique of Western blot (Fig. 7A), PMA stimulation induced the accumulation of β-catenin in the membrane fraction concomitant with a decrease in the soluble fraction. Immunostaining of β-catenin in cells transiently transfected with hPKCα-wt–GFP showed (Fig. 7B) that, in basal conditions, β-catenin was detected both in the cytoplasm and at the plasma membrane. PMA stimulation induced a redistribution of β-catenin staining: β-catenin levels increased at the interface of apposed cells, where hPKCα-wt–GFP accumulation also occurred, at the expense of staining of the re-
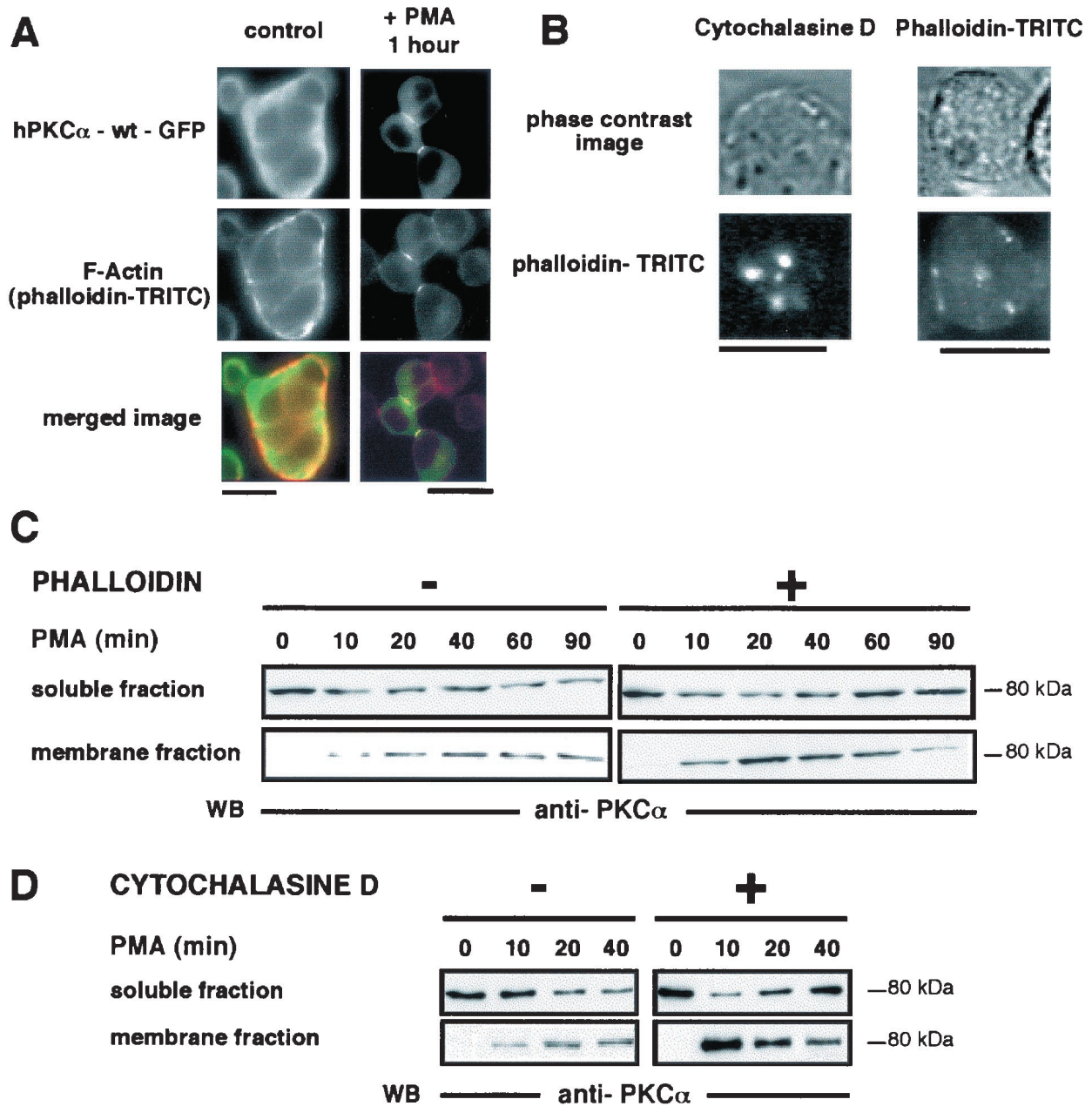
FIG. 5. Upon PMA stimulation, the reorganization of F-actin at the cell-cell contacts is necessary for PKCα accumulation at the interface between apposed cells. (A) GH3B6 cells transfected with hPKCα-wt–GFP (top) were analyzed for F-actin localization by immunocytochemistry using phalloidin-TRITC (bottom) in basal conditions (left) and after 1 h of PMA treatment (right). In basal conditions, F-actin was uniformly found at the plasma membrane, whereas hPKCα-wt–GFP was cytoplasmic. Upon PMA stimulation, F-actin and hPKCα-wt–GFP accumulated concomitantly at the cell-cell contacts. Merged image: green, hPKCα-wt–GFP; red, phalloidin-TRITC. (B) Disorganization of F-actin network. Cells preincubated with 0.5 μM cytochalasin D for 30 min (left) were fixed and labeled with phalloidin-TRITC. As expected, the F-actin network was disrupted by this drug treatment as evidenced by the presence of spots. Cells were incubated with phalloidin-TRITC for 1 h (right). In these conditions, phalloidin-TRITC staining was seen in the cells as spots, indicating that the F-actin network has been disorganized. Bars, 5 μm. (C and D) Western blot analysis, using an anti-PKCα antibody, of PKCα translocation and accumulation induced by PMA stimulation in GH3B6 cells incubated or not for 1 h with 10^{-5} M phalloidin (C) or for 30 min with 0.5 μM cytochalasin D (D). In basal conditions, in the presence or in the absence of phalloidin or cytochalasin D, PKCα is mainly cytoplasmic. When cells are not incubated with phalloidin or cytochalasin D, PMA treatment induced the translocation and persistent accumulation (90 min) of PKCα to the membrane fraction. (C) When cells are preincubated with phalloidin before PMA treatment, the PKCα amount increased in the membrane fraction before decreasing. The soluble fraction recovered its basal level after 90 min of PMA treatment. As shown in panel D, similar results were obtained when cells were preincubated with cytochalasin D prior to PMA treatment.
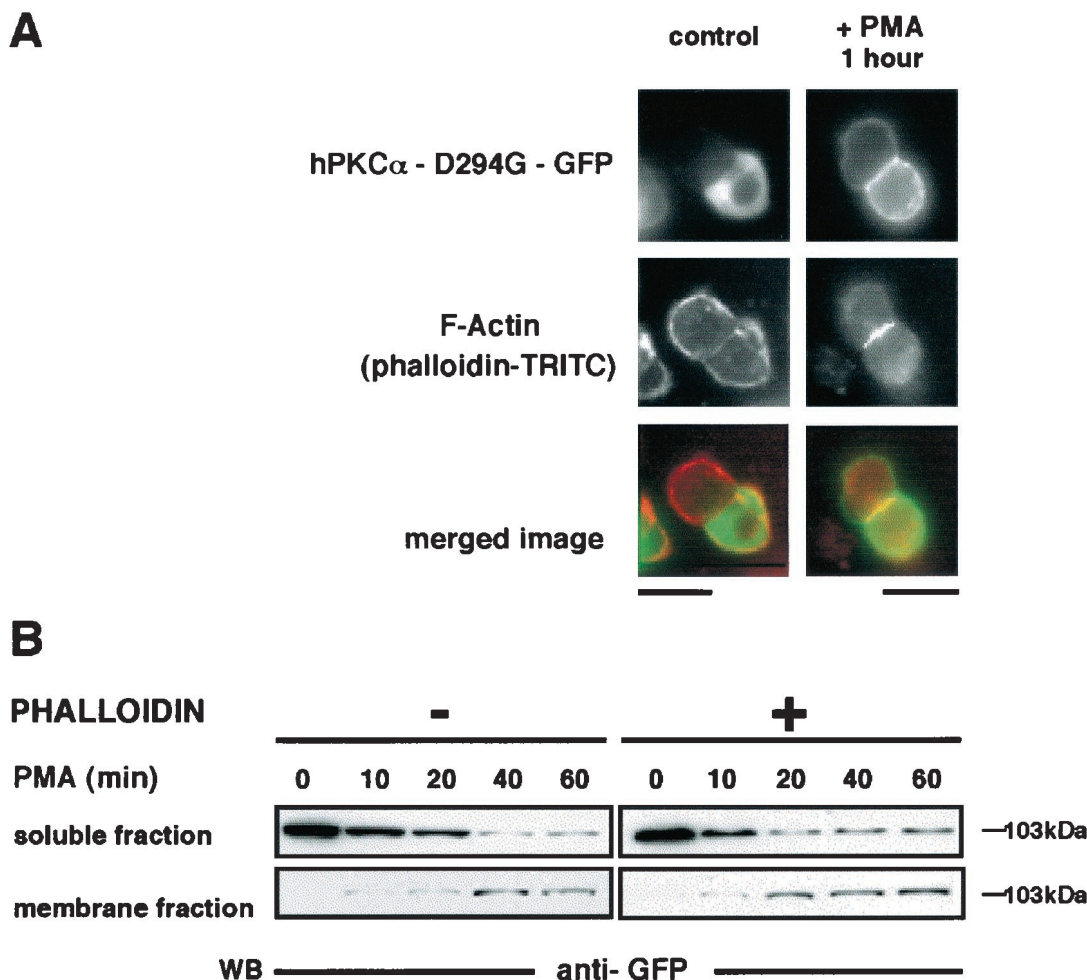
FIG. 6. Upon PMA stimulation, the accumulation of hPKCα-D294G at the plasma membrane does not depend on the reorganization of F-actin. (A) GH3B6 cells transfected with hPKCα-D294G–GFP (top) were analyzed for F-actin localization by immunocytochemistry by using phalloidin-TRITC (bottom) in basal conditions (left) and after 1 h of PMA treatment (right). In basal conditions, F-actin was uniformly found at the plasma membrane, whereas hPKCα-D294G–GFP was cytoplasmic. Upon PMA stimulation, F-actin accumulated at the cell-cell contacts, whereas hPKCα-D294G–GFP translocated uniformly at the plasma membrane. Merged image: green, hPKCα-D294G–GFP; red, phalloidin-TRITC. Bar, 5 μm. (B) Western blot analysis, using an anti-GFP antibody, of hPKCα-D294G–GFP translocation and accumulation induced by PMA stimulation in GH3B6 cells incubated or not with phalloidin. The results show that the disorganization of the F-actin network affects neither the translocation nor the accumulation of hPKCα-D294G–GFP.

maining part of the plasma membrane and cytoplasm. We then investigated whether the aberrant hPKCα-D294G–GFP localization was associated with a different β-catenin subcellular distribution. Figure 7C shows that this is not the case: in cells transiently transfected with hPKCα-D294G–GFP, β-catenin still accumulated at the cell-cell contacts.

We have shown above that disrupting the F-actin network prevents the accumulation of hPKCα at the cell-cell contacts. Is β-catenin localization also affected by the disruption of the microfilament network? The results of β-catenin immunostaining in cells treated with cytochalasin D and PMA (1 h of treatment) shows that this is the case (Fig. 7D). Shorter PMA treatments (10 and 30 min) gave identical results (data not shown). Reorganization of the F-actin network at the cell-cell contacts upon PMA treatment is therefore necessary for β-catenin to accumulate at these cell-cell contacts.

Long-term TRH stimulation induces F-actin and β-catenin accumulation at the cell-cell contacts. In GH3B6 cells, TRH

induces a biphasic accumulation of hPKCα at the plasma membrane, the second phase being abolished by deletion of the V1 region, as is the PMA-induced translocation (42). However, in order to assess whether F-actin reorganization and β-catenin relocalization at the cell-cell contacts are induced upon long-term TRH treatment, as they are after PMA treatment, GH3B6 cells were treated for 2 h with 100 nM TRH. As shown in Fig. 8, this 2-h treatment had the same effects as the PMA treatment: it induced F-actin reorganization at the cell-cell contacts and induced β-catenin accumulation. Therefore, long-term physiological stimulation has effects also encountered upon treatment with PMA, which is considered a pharmacological, nonphysiological PKC activator.

DISCUSSION

The present study was initiated by the observation that hPKCα is selectively targeted to cell-cell contacts in TRH- or

A

WB ——— anti-β-catenin ———

B

C

D
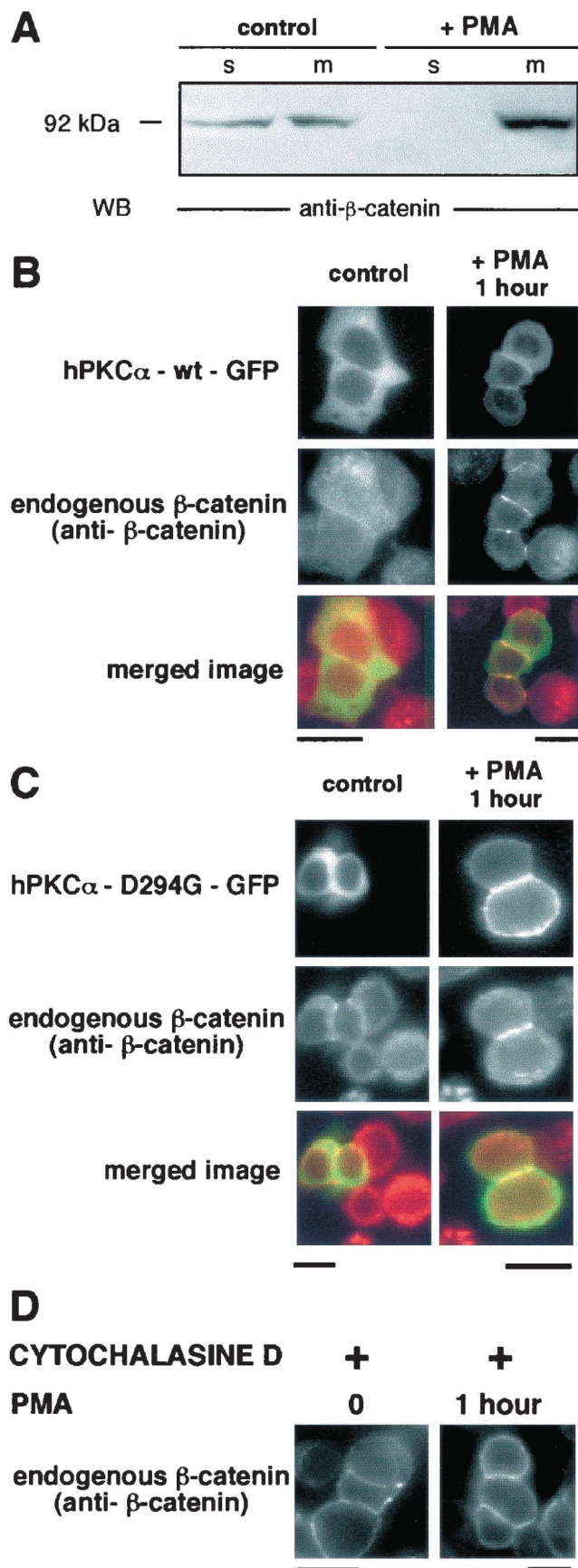
PMA-treated GH3B6 cells. Since both PKC and cell adhesion are involved in complex biological processes such as development and oncogenic transformation, we considered them to be of potential importance for improving our understanding of hPKCα targeting to cell-cell contacts. The results presented here and, in particular, the fact that a natural mutation of hPKCα abolishes the specific accumulation of the kinase at sites of cell-cell contact, led us to consider hPKCα as an active player in the control of pituitary intercellular communication via cell adhesion.

hPKCα targeting at cell-cell contacts: a regulated mechanism. Targeting of a protein is a complex phenomenon that requires an understanding of its spatiotemporal dynamic. According to our previous study (42), hPKCα spatiotemporal dynamic is constituted by two translocation phases upon TRH physiological stimulation: a rapid and transient phase, followed by a slow and long-lasting phase. Both phases involve different translocation mechanisms since deletion of the V1 region of hPKCα abolishes the second phase without affecting the first one. Upon PMA stimulation, there is one long-lasting translocation phase which exhibits similarities with the second phase of translocation upon TRH treatment since what affects it also affects the second translocation phase upon TRH and vice versa (42). Based on the results presented here, we now know also that the selectivity of the targeting site, which is the same whatever the translocation phase and the stimulus, is highly controlled. A single point mutation localized in the hinge region of hPKCα, at position 294, is sufficient to affect it. One possible explanation is that the D294G mutation, localized in the V3 region that is not directly involved in the interaction with diacylglycerol, Ca^{2+}, or phosphatidylserine, specifically abolishes the interaction of PKCα with one or several cytoplasmic chaperone proteins whose mission is to bring PKCα to the regions of cell-cell contacts. Indeed, we have previously shown (32) that the hPKCα-D294G mutant is no longer able to interact with substrates with anchoring protein properties. Also supporting this hypothesis is the fact that the hinge V3 region is involved with the C2 calcium binding region in the

FIG. 7. Upon PMA stimulation, β-catenin accumulates at the cell-cell contacts. (A) Western blot analysis of β-catenin distribution. Soluble (s) and membrane (m) fractions of untreated or PMA-treated GH3B6 cells were subjected to SDS-PAGE and Western blotting using an anti-β-catenin antibody. In basal conditions, β-catenin was found in soluble and membrane fractions. PMA treatment induced β-catenin accumulation in the membrane fraction. (B and C) GH3B6 cells transfected with hPKCα-wt–GFP (B, top) or hPKCα-D294G–GFP (C, top) were analyzed for β-catenin localization by immunocytochemistry with an anti-β-catenin antibody (B and C, bottom) in basal conditions (left) and after 1 h of PMA treatment (right). In basal conditions, β-catenin immunoreactivity was found in the cytoplasm and at the plasma membrane, whereas hPKCα-wt–GFP and hPKCα-D294G–GFP were cytoplasmic. PMA stimulation induced the redistribution of β-catenin to cell-cell contacts. Merged image: green, hPKCα-wt–GFP or hPKCα-D294G–GFP; red, β-catenin. (D) Accumulation of β-catenin at the cell-cell contacts induced by PMA treatment depends on the reorganization of F-actin at the cell-cell contacts. Immunostaining of β-catenin of cells treated with cytochalasin D in the absence or in the presence of 100 nM PMA. In the presence of cytochalasin D, β-catenin is no more accumulated at the cell-cell contacts upon PMA stimulation. Bars, 5 μm.
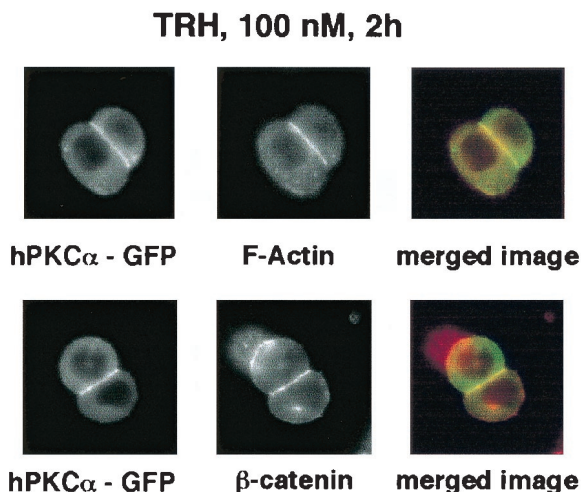
TRH, 100 nM, 2h

hPKCα - GFP F-Actin merged image

hPKCα - GFP β-catenin merged image

FIG. 8. After 2 h of TRH stimulation, F-actin and β-catenin accumulate at the cell-cell contacts. GH3B6 cells transfected with hPKCα-wt–GFP were analyzed for F-actin and β-catenin localization by immunocytochemistry using phalloidin-TRITC and an anti-β-catenin antibody. Cells were treated for 2 h with 100 nM TRH. Merged image: green, hPKCα-wt–GFP; red, either F-actin (top) or β-catenin (bottom).

cytoplasmic sequestration of hPKCα, probably via binding to a cytoplasmic anchoring protein (42).

Which role for calcium in hPKCα targeting? Spatiotemporal localization of a protein can be devided into two events: translocation from one subcellular compartment to another and accumulation at the targeting site. It is generally accepted that translocation of conventional PKCs, among which is the α isoform, requires calcium and that calcium is sufficient to induce translocation (1, 8, 26). We have shown that, in GH3B6 cells, this is not the case since hPKCα-wt does not translocate (first translocation phase) in isolated cells despite the rise in $[Ca^{2+}]_i$ as in apposed cells (42) observed upon physiological stimulation. In the present study, we provide evidence that the accumulation of the kinase at cell-cell contacts that occurs during the first phase of translocation may be also independent of the $[Ca^{2+}]_i$. Indeed, wild-type hPKCα returns to the cytoplasm despite a still-elevated calcium concentration in the cell. Under the same conditions, the D294G mutant remains at the plasma membrane and stays there as long as the $[Ca^{2+}]_i$ is high. The mutant behaves in GH3B6 cells the same way PKCγ behaves in rat basophilic leukemia 2H3 cells (26): translocation follows variations in intracellular calcium concentrations. PKCγ is a brain-specific PKC isoform. Rat basophilic leukemia 2H3 cells may not have provided the adequate binding partners for PKCγ to be adequately targeted the way PKCα is targeted in GH3B6 cells. As suggested above, the D294G mutant probably may no longer recognize a cytoplasmic protein involved in targeting of the wild-type enzyme and, when targeting of PKC becomes independent of isoform-specific binding partners, it might only be dependent upon variations in $[Ca^{2+}]_i$. Also, the fact that when the $[Ca^{2+}]_i$ decreases, the mutant dissociates from the plasma membrane supports its direct interaction with phospholipids. Indeed, previous studies have shown that the interaction of PKC with phospholipidic vesicles is rapidly disrupted in the presence of a calcium chelator (25). In contrast, the fact that the wild-type enzyme returns to the cytoplasm despite elevated calcium concentrations suggests a mode of interaction of PKCα with the plasma membrane at the cell-cell contacts which probably involves a direct interaction with anchoring proteins even though we cannot rule out the fact that it may still require elevated $[Ca^{2+}]_i$.

RACK1 is not an hPKCα anchoring protein in GH3B6 cells. The natural mutation of hPKCα located in the V3 hinge region abolishes the specific accumulation of the kinase at sites of cell-cell contact (42) by inducing hPKCα targeting to the entire plasma membrane, including cell-cell contacts. As stated above, one possible explanation for this fact is that the D294G mutation specifically abolishes the interaction of PKCα with one or several cytoplasmic chaperones. To test this hypothesis, we investigated the putative role of RACK1, which was the first PKC anchoring protein to be isolated (24, 33) and was subsequently shown to bind several PKC isoforms, including βII, ε, and α (35, 36, 46). In unstimulated and long-term TRH- or PMA-stimulated GH3B6 cells, however, we could never detect RACK1 at the cell-cell contacts. In addition, we found that RACK1 and hPKCα-wt, although colocalized in the cytoplasm, never coimmunoprecipitated whether cells were treated or not with PMA. Similar results were obtained with the D294G mutant, despite its colocalization with RACK1 at plasma membrane sites other than the cell-cell contacts, upon PMA treatment of cells. On the basis of these results, we concluded that RACK1 does not mediate translocation nor accumulation of either wild-type or D294G hPKCα under PMA stimulation.

F-actin network is involved in accumulation of PKCα at the cell-cell contacts. In the present study, we show that upon PMA treatment or long-term TRH stimulation, there is a concentration of F-actin at the cell-cell contacts of all apposed cells, whereas the translocation of PKCα occurs only in a subpopulation of these cells (42). Hence, translocation of PKCα is not what causes the reorganization of the F-actin network. In GH3B6 cells, PMA does not affect the $[Ca^{2+}]_i$ (unpublished results), although it induces the growth of actin filaments at the cell-cell contacts. This indicates that, unlike the synaptic terminal of retinal bipolar cells where PMA increases the growth of actin filaments only in the presence of a Ca^{2+} influx (17), the PMA-induced F-actin network reorganization may involve activation of a calcium-independent PKC. Our present study showing that the translocation of PKCα is maintained in cytochalasin D- or phalloidin-treated GH3B6 cells argues against F-actin playing an active role during translocation. This contrasts with another report showing that nuclear translocation of PKCα in NIH 3T3 fibroblasts depends on the integrity of the cytoskeleton (37), but it is in line with the observed PMA-induced translocation of PKCα in cytochalasin D-treated C6 glioma cells (9). Interestingly, we found that long-lasting accumulation of PKCα at the plasma membrane cannot occur but that the kinase returns to the cytoplasm in phalloidin- or cytochalasin D-treated GH3B6 cells. This does indicate a role of F-actin in the mechanism by which PKCα remains localized at the cell-cell contacts, in the vicinity of its substrates. The interaction between PKCα and F-actin at the cell-cell contacts could be direct or indirect. Like PKCζ (10), PKCβII, and PKCε (7, 30), PKCα could directly interact with F-actin at the cell-cell contacts. An example of indirect interaction with F-actin is given by the cyclic-AMP-dependent protein kinase IIβ,

which is also linked to the actin cytoskeleton in both neurons (22) and non-neuron cells (21). Rather than a direct binding to F actin, in this case the kinase is linked to the cytoskeleton by the kinase anchor protein AKAP75. Furthermore, F-actin might be required to stimulate PKCα activity in order for PKCα to phosphorylate its substrate at the cell-cell contacts since it has been shown to directly stimulate PKC activity (39). Since when the F-actin network is disrupted the intact PKCα returns to the cytoplasm, the integrity of the F-actin network could be required for PKCα to be downregulated.

Concerning the D294G mutant, its accumulation at the plasma membrane does not require the integrity of the F-actin network. This supports the hypothesis described above that the interaction between the mutant and the plasma membrane is mediated through a direct interaction with phospholipids.

The PMA-induced F-actin network organization at cell-cell contacts implies depolymerization of the filaments at the plasma membrane and exclusive repolymerization at the cell-cell contacts. A recent result suggests that the actin cytoskeleton may itself be part of the intracellular Ca^{2+} store (20). Despite the large differences in bulk concentrations of intracellular free Mg^{2+} and Ca^{2+}, the probability that actin subunits near the membrane bind Ca^{2+} and then incorporate into filaments would allow accumulation of several micromolar Ca^{2+} in the near-millimolar pool of actin. This pool of Ca^{2+} would be released when the actin depolymerizes. Moreover, changes in discrete subcellular Ca^{2+} pools in response to diverse stimuli may be more relevant to the targeting and accumulation of various PKC isoforms than changes in the bulk concentration of Ca^{2+}. This mechanism could be involved in a calcium-dependent association of PKC with the membrane and, in particular, in that of the hPKCα mutant.

Which role for PKCα at the cell-cell contacts? Several examples in the literature argue in favor of a biological significance of the interaction between PKC and F-actin, hence arguing in favor of a biological significance of the interaction between PKCα and F-actin at the GH3B6 cell-cell contacts. Among these examples, PKCζ translocates to and stabilizes the actin network after stimulation by interleukin-2 (10), and this association is also required for glutamate release in PMA-treated neuronal cells (41).

The presence of PKCα at the cell-cell contacts led us to search for the presence of putative protein substrates of PKCα at this location, and we thought of β-catenin as a potential candidate. β-Catenin is known for its interaction with E-cadherins, which mediate intercellular adhesion. In unstimulated GH3B6 cells, we found β-catenin both at the plasma membrane and in the cytoplasm, whereas PMA treatment or long-term TRH stimulation induced a concentration of β-catenin at the cell-cell contacts, concomitantly with F-actin and hPKCα. In contrast to PKCα, the concentration of β-catenin was observed in all apposed cells, demonstrating that PKCα is not the causative agent of β-catenin accumulation at the cell-cell contacts. In cytochalasin D-treated cells, β-catenin no longer concentrates at the cell-cell contacts, whereas PKCα does; this result suggests that β-catenin is not the causative agent of PKCα targeting at the cell-cell contacts. Up to now, we did not succeed in coimmunoprecipitating β-catenin and PKCα nor in showing a serine-threonine phosphorylation of β-catenin upon PMA stimulation (data not shown). We thus do not know if there is a functional link between β-catenin and PKCα that could account for the accumulation of PKCα at the cell-cell contacts. Further work is thus needed to investigate which protein(s) is able to interact with PKCα at the cell-cell contact. Their identification will help us understand the physiopathological consequences of the loss of PKCα targeting at the cell-cell contacts by the D294G point mutation and thus the physiological relevance of this mutant in tumorigenesis. Up to now, there is no clear evidence that this mutant is important in cell transformation. A large-scale analysis of the relationships between the presence of the mutant and the tumor phenotypes should be done in order to clarify the potential interest of this mutation and, beyond this mutation, analysis of the presence of other mutations in the hPKCα gene should be undertaken. In addition, the hPKCα gene is located in a particularly interesting region of chromosome 17, q23-q24. Chromosome 17q is frequently rearranged in breast cancers in which we have detected the D294G point mutation (unpublished data), and gains with DNA amplification are most commonly observed in the 17q23–q24 regions (27). This indicates that the relationship between PKCα and tumorigenesis could be of at least two types: (i) amplification of the wild-type gene, leading to overexpression of the wild-type protein, and (ii) the possible presence of genomic abnormalities, among which are point mutations. Interestingly, altered forms of PKCα have been observed in two cell lines. A smaller-than-expected PKCα was found in a small lung carcinoma cell line (57 kDa instead of 80 kDa), probably resulting from an aberrant posttranslational processing of the protein (18), and a tumor-specific deletion within the gene encoding PKCα was found in a primary melanoma cell line (23).

In conclusion, by showing that a single point mutation known to be without intrinsic effect on catalytic activity can abolish targeting selectivity, the present study highlights the complexity of PKCα regulation and reinforces the necessity to consider PKC signaling as a network of interacting events rather than as a linear chain of interactions.

REFERENCES

1. **Almholt, K., P. O. Arkhammar, O. Thastrup, and S. Tullin.** 1999. Simultaneous visualization of the translocation of protein kinase Calpha-green fluorescent protein hybrids and intracellular calcium concentrations. Biochem. J. **337:**211–218.
2. **Alvaro, V., L. Levy, C. Dubray, A. Roche, F. Peillon, B. Querat, and D. Joubert.** 1993. Invasive human pituitary tumors express a point-mutated alpha-protein kinase-C. J. Clin. Endocrinol. Metab. **77:**1125–1129.
3. **Alvaro, V., C. Prevostel, D. Joubert, E. Slosberg, and B. I. Weinstein.** 1997. Ectopic expression of a mutant form of PKCalpha originally found in human tumors: aberrant subcellular translocation and effects on growth control. Oncogene **14:**677–685.
4. **Aplin, A. E., A. K. Howe, and R. L. Juliano.** 1999. Cell adhesion molecules, signal transduction and cell growth. Curr. Opin. Cell. Biol. **11:**737–744.
5. **Baciu, P. C., and P. F. Goetinck.** 1995. Protein kinase C regulates the

recruitment of syndecan-4 into focal contacts. Mol. Biol. Cell **6:**1503–1513.

6. **Battaini, F., A. Pascale, R. Paoletti, and S. Govoni.** 1997. The role of anchoring protein RACK1 in PKC activation in the ageing rat brain. Trends Neurosci. **20:**410–415.

7. **Blobe, G. C., D. S. Stribling, D. Fabbro, S. Stabel, and Y. A. Hannun.** 1996. Protein kinase C beta II specifically binds to and is activated by F- actin. J. Biol. Chem. **271:**15823–15830. (Erratum, **271:**30297.)

8. **Corbalan-Garcia, S., J. A. Rodriguez-Alfaro, and J. C. Gomez-Fernandez.** 1999. Determination of the calcium-binding sites of the C2 domain of protein kinase Calpha that are critical for its translocation to the plasma membrane. Biochem. J. **337:**513–521.

9. **Douglas, D. N., H. S. Fink, S. D. Rose, N. D. Ridgway, H. W. Cook, and D. M. Byers.** 1997. Inhibitors of actin polymerization and calmodulin binding enhance protein kinase C-induced translocation of MARCKS in C6 glioma cells. Biochim. Biophys. Acta **1356:**121–130.

10. **Gomez, J., A. Martinez de Aragon, P. Bonay, C. Pitton, A. Garcia, A. Silva, M. Fresno, F. Alvarez, and A. Rebollo.** 1995. Physical association and functional relationship between protein kinase C zeta and the actin cytoskeleton. Eur. J. Immunol. **25:**2673–2678.

11. **Goode, N., K. Hughes, J. R. Woodgett, and P. J. Parker.** 1992. Differential regulation of glycogen synthase kinase-3 beta by protein kinase C isotypes. J. Biol. Chem. **267:**16878–16882.

12. **Guérineau, N. C., X. Bonnefont, L. Stoeckel, and P. Mollard.** 1998. Synchronized spontaneous Ca^{2+} transients in acute anterior pituitary slices. J. Biol. Chem. **273:**10389–10395.

13. **Hagmann, J., and M. M. Burger.** 1992. Phosphorylation of vinculin in human platelets spreading on a solid surface. J. Cell Biochem. **50:**237–244.

14. **Horowitz, A., and M. Simons.** 1998. Phosphorylation of the cytoplasmic tail of syndecan-4 regulates activation of protein kinase Calpha. J. Biol. Chem. **273:**25548–25551.

15. **Horowitz, A., and M. Simons.** 1998. Regulation of syndecan-4 phosphorylation in vivo. J. Biol. Chem. **273:**10914–10918.

16. **Ikeda, S., S. Kishida, H. Yamamoto, H. Murai, S. Koyama, and A. Kikuchi.** 1998. Axin, a negative regulator of the Wnt signaling pathway, forms a complex with GSK-3beta and beta-catenin and promotes GSK-3beta-dependent phosphorylation of beta-catenin. EMBO J. **17:**1371–1384.

17. **Job, C., and L. Lagnado.** 1998. Calcium and protein kinase C regulate the actin cytoskeleton in the synaptic terminal of retinal bipolar cells. J. Cell Biol. **143:**1661–1672.

18. **Jones, C. L., L. K. Beck, J. P. Brozna, M. Holley, E. J. Dempsey, and M. A. Kane.** 1995. Properties of classic protein kinase C in human small cell lung carcinoma NCI-H345 cells. Cell Growth Differ. **6:**1627–1634.

19. **Laemmli, U. K.** 1970. Cleavage of structural proteins during the assembly of the head of bacteriophage T4. Nature **227:**680–685.

20. **Lange, K., and U. Brandt.** 1996. Calcium storage and release properties of F-actin: evidence for the involvement of F-actin in cellular calcium signaling. FEBS Lett. **395:**137–142.

21. **Li, Y., C. Ndubuka, and C. S. Rubin.** 1996. A kinase anchor protein 75 targets regulatory (RII) subunits of cAMP-dependent protein kinase II to the cortical actin cytoskeleton in non-neuronal cells. J. Biol. Chem. **271:** 16862–16869.

22. **Li, Y., and C. S. Rubin.** 1995. Mutagenesis of the regulatory subunit (RII beta) of cAMP-dependent protein kinase II beta reveals hydrophobic amino acids that are essential for RII beta dimerization and/or anchoring RII beta to the cytoskeleton. J. Biol. Chem. **270:**1935–1944.

23. **Linnenbach, A. J., K. Huebner, E. P. Reddy, M. Herlyn, A. H. Parmiter, P. C. Nowell, and H. Koprowski.** 1988. Structural alteration in the MYB proto-oncogene and deletion within the gene encoding alpha-type protein kinase C in human melanoma cell lines. Proc. Natl. Acad. Sci. USA **85:**74–78.

24. **Mochly-Rosen, D., H. Khaner, and J. Lopez.** 1991. Identification of intracellular receptor proteins for activated protein kinase C. Proc. Natl. Acad. Sci. USA **88:**3997–4000.

25. **Mosior, M., and A. C. Newton.** 1995. Mechanism of interaction of protein kinase C with phorbol esters. Reversibility and nature of membrane association. J. Biol. Chem. **270:**25526–25533.

26. **Oancea, E., and T. Meyer.** 1998. Protein kinase C as a molecular machine for decoding calcium and diacylglycerol signals. Cell **95:**307–318.

27. **Orsetti, B., F. Courjal, M. Cuny, C. Rodriguez, and C. Theillet.** 1999. 17q21–

28. **Pauken, C. M., and D. G. Capco.** 1999. Regulation of cell adhesion during embryonic compaction of mammalian embryos: roles for PKC and beta-catenin. Mol. Reprod. Dev. **54:**135–144.

29. **Perez-Moreno, M., A. Avila, S. Islas, S. Sanchez, and L. Gonzalez-Mariscal.** 1998. Vinculin but not alpha-actinin is a target of PKC phosphorylation during junctional assembly induced by calcium. J. Cell Sci. **111:**3563–3571.

30. **Prekeris, R., R. M. Hernandez, M. W. Mayhew, M. K. White, and D. M. Terrian.** 1998. Molecular analysis of the interactions between protein kinase C-epsilon and filamentous actin. J. Biol. Chem. **273:**26790–26798.

31. **Prevostel, C., V. Alvaro, F. de Boisvilliers, A. Martin, C. Jaffiol, and D. Joubert.** 1995. The natural protein kinase C alpha mutant is present in human thyroid neoplasms. Oncogene **11:**669–674.

32. **Prevostel, C., V. Alvaro, A. Vallentin, A. Martin, S. Jaken, and D. Joubert.** 1998. Selective loss of substrate recognition induced by the tumour-associated D294G point mutation in protein kinase Calpha. Biochem. J. **334:**393–397.

33. **Ron, D., C. H. Chen, J. Caldwell, L. Jamieson, E. Orr, and D. Mochly-Rosen.** 1994. Cloning of an intracellular receptor for protein kinase C: a homolog of the beta subunit of G proteins. Proc. Natl. Acad. Sci. USA **91:**839–843. (Erratum, **92:**2016, 1995.)

34. **Ron, D., Z. Jiang, L. Yao, A. Vagts, I. Diamond, and A. Gordon.** 1999. Coordinated movement of RACK1 with activated betaIIPKC. J. Biol. Chem. **274:**27039–27046.

35. **Ron, D., J. Luo, and D. Mochly-Rosen.** 1995. C2 region-derived peptides inhibit translocation and function of beta protein kinase C in vivo. J. Biol. Chem. **270:**24180–24187.

36. **Rotenberg, S. A., and X. G. Sun.** 1998. Photoinduced inactivation of protein kinase C by dequalinium identifies the RACK-1-binding domain as a recognition site. J. Biol. Chem. **273:**2390–2395.

37. **Schmalz, D., F. Kalkbrenner, F. Hucho, and K. Buchner.** 1996. Transport of protein kinase C alpha into the nucleus requires intact cytoskeleton while the transport of a protein containing a canonical nuclear localization signal does not. J. Cell Sci. **109:**2401–2406.

38. **Schwienbacher, C., B. M. Jockusch, and M. Rudiger.** 1996. Intramolecular interactions regulate serine/threonine phosphorylation of vinculin. FEBS Lett. **384:**71–74.

39. **Slater, S. J., S. K. Milano, B. A. Stagliano, K. J. Gergich, J. P. Curry, F. J. Taddeo, and C. D. Stubbs.** 2000. Interaction of protein kinase C with filamentous actin: isozyme specificity resulting from divergent phorbol ester and calcium dependencies. Biochemistry **39:**271–280.

40. **Steinberg, M. S., and P. M. McNutt.** 1999. Cadherins and their connections: adhesion junctions have broader functions. Curr. Opin. Cell Biol. **11:**554–560.

41. **Terrian, D. M., and D. K. Ways.** 1995. Persistent enhancement of sustained calcium-dependent glutamate release by phorbol esters: role of calmodulin-independent serine/threonine phosphorylation and actin disassembly. J. Neurochem. **64:**181–190.

42. **Vallentin, A., C. Prevostel, T. Fauquier, X. Bonnefont, and D. Joubert.** 2000. Membrane targeting and cytoplasmic sequestration in the spatiotemporal localization of human protein kinase C alpha. J. Biol. Chem. **275:**6014–6021.

43. **van Hengel, J., L. Gohon, E. Bruyneel, S. Vermeulen, M. Cornelissen, M. Mareel, and F. von Roy.** 1997. Protein kinase C activation upregulates intercellular adhesion of alpha-catenin-negative human colon cancer cell variants via induction of desmosomes. J. Cell Biol. **137:**1103–1116.

44. **Vasioukhin, V., C. Bauer, M. Yin, and E. Fuchs.** 2000. Directed actin polymerization is the driving force for epithelial cell-cell adhesion. Cell **100:**209–219.

45. **Weekes, J., S. T. Barry, and D. R. Critchley.** 1996. Acidic phospholipids inhibit the intramolecular association between the N- and C-terminal regions of vinculin, exposing actin-binding and protein kinase C phosphorylation sites. Biochem. J. **314:**827–832.

46. **Yedovitzky, M., D. Mochly-Rosen, J. A. Johnson, M. O. Gray, D. Ron, E. Abramovitch, E. Cerasi, and R. Nesher.** 1997. Translocation inhibitors define specificity of protein kinase C isoenzymes in pancreatic beta-cells. J. Biol. Chem. **272:**1417–1420.

q25 aberrations in breast cancer: combined allelotyping and CGH analysis reveals 5 regions of allelic imbalance among which two correspond to DNA amplification. Oncogene **18:**6262–6270.